CPC(HEP & NP), 2010, **34**(9): 1421–1424 Chinese Physics C Vol. 34, No. 9, Sep., 2010

Comparing AdS/CFT dipole model to HERA F_2 data*

LÜ Zhun(吕准)[1,2]

[1] Department of Physics, Southeast University, Nanjing, China
[2] Departamento de Física y Centro de Estudios Subatómicos,
Universidad Técnica Federico Santa María, Casilla 110-V, Valparaíso, Chile

Abstract We apply an AdS/CFT-inspired color-dipole model which contains only three free parameters to describe the HERA data for the inclusive structure function F_2 at small Bjorken-x and virtuality. We found that the saturation scale in our AdS/CFT-based parameterization varies in the range of $1 \div 3$ GeV becoming independent of energy/Bjorken-x at very small x. This leads to the prediction of x-independence of the structure functions at very small x. With the fitted parameters in our model, the predictions for F_2, longitudinal structure function, charm structure function and total photo-production cross-sections in the kinematic regions of future experiments can be given.

Key words color dipole model, AdS/CFT correspondence, structure function, saturation scale

PACS 24.85.+p, 25.75.-q, 12.38.Mh

1 Introduction

One of the most valuable tools for the exploration of QCD is the measurement of the proton structure function in deep inelastic scattering (DIS) at small Bjorken-x. For sufficiently high energies/small Bjorken-x, perturbative QCD predicts that gluons in a hadron wavefunction form a Color Glass Condensate (CGC) [1–3]. The main principle of the CGC is the existence of a hard saturation scale Q_s at which nonlinear gluons recombination effects start to become important. The saturation scale Q_s grows rapidly with energy or according to the perturbative nonlinear Balitsky-Kovchegov (BK) [2] and Jalilian-Marian–Iancu–McLerran–Weigert–Leonidov–Kovner (JIMWLK) [3] evolution equations. In the leading logarithmic $(\ln 1/x)$ approximation at fixed coupling, the BK equation predicts that ${Q_s}^2(x) \sim (1/x)^{4.6\ \alpha_s}$ [4], which is a much faster growth of the saturation scale than one expects from HERA data. One possible way to constrain higher order corrections to those equations is to consider small-x evolution in the large coupling limit. In light of this, one may resort to other QCD-like theories, such as $\mathcal{N}=4$ super Yang-Mills (SYM) theory where one can perform calculations in the non-perturbative limit of large 't Hooft coupling by employing the Anti-de Sitter space/conformal field theory (AdS/CFT) correspondence [5].

Recently, the authors of [6] calculated the total cross-section for a quark dipole scattering on a nucleus at high energy for a strongly coupled $\mathcal{N}=4$ SYM theory using AdS/CFT correspondence. The forward scattering amplitude for the $q\bar{q}$ dipole-nucleus scattering was derived in [6] and exhibited an interesting feature: at high energy the amplitude would stop growing with energy, becoming a constant. Here we will confront the color-dipole scattering amplitude on a nucleus from the AdS/CFT correspondence [6] with the available HERA data. Given the non-perturbative nature of the AdS/CFT approach, we expect this model to be valid at small x but also at small Q^2 where the experimental data are very limited. Below we show that the HERA data for the inclusive structure function F_2 at very small x and Q^2 can be well described within the color dipole picture inspired by the AdS/CFT approach [6]. We show that, unlike the perturbative predictions for its behavior, the saturation scale from the AdS/CFT approach becomes independent of energy/Bjorken-x at very high energy. This leads to the x-independent behavior of the structure function F_2 at very small x

Received 19 January 2010
* Supported by PBCT Project (ACT/028 "Center of Atomic Physics") and FONDECYT (Chile) Project (11090085)

and Q^2.

2 Color dipole description of structure function F_2

The DIS cross sections at small x can be described by the color dipole factorization scheme:

$$\sigma_{\mathrm{L,T}}^{\gamma^*\mathrm{p}}(Q^2,x)= \sum_{\mathrm{f}}\int \mathrm{d}^2 r\int_0^1 \mathrm{d}z\, |\Psi_{\mathrm{L,T}}^{(\mathrm{f})}(r,z;Q^2)|^2\,\sigma_{\mathrm{q\bar{q}}}(r,x), \quad (1)$$

here $\sigma_{\mathrm{q\bar{q}}}(r,x)$ denotes the $\mathrm{q\bar{q}}$ dipole-proton scattering cross-section incorporating QCD effects, and the light-cone wavefunction $\Psi_{\mathrm{L,T}}^{(\mathrm{f})}$ for $\gamma^\star$ can be expressed as [7]:

$$|\Psi_{\mathrm{T}}^{(\mathrm{f})}(r,z;Q^2)|^2 = \frac{\alpha N_{\mathrm{c}}}{2\pi^2}\sum_{\mathrm{f}} e_{\mathrm{f}}^2\,\{a_{\mathrm{f}}^2[K_1(ra_{\mathrm{f}})]^2\times [z^2+(1-z)^2]+m_{\mathrm{f}}^2[K_0(ra_{\mathrm{f}})]^2\}, \quad (2)$$

$$|\Psi_{\mathrm{L}}^{(\mathrm{f})}(r,z;Q^2)|^2 = \frac{\alpha N_{\mathrm{c}}}{2\pi^2}\sum_{\mathrm{f}} e_{\mathrm{f}}^2\,\{4Q^2z^2(1-z)^2\times [K_0(r\,a_{\mathrm{f}})]^2\}. \quad (3)$$

The proton structure function F_2 and the longitudinal structure function F_{L} can be written in terms of $\gamma^\star$p cross-section,

$$F_2(Q^2,x) = \frac{Q^2}{4\pi^2\alpha}\left[\sigma_{\mathrm{L}}^{\gamma^*\mathrm{p}}(Q^2,x)+\sigma_{\mathrm{T}}^{\gamma^*\mathrm{p}}(Q^2,x)\right], \quad (4)$$

$$F_{\mathrm{L}}(Q^2,x) = \frac{Q^2}{4\pi^2\alpha}\sigma_{\mathrm{L}}^{\gamma^*\mathrm{p}}(Q^2,x). \quad (5)$$

The contribution of the charm quark to the wave functions in Eqs. (2) and (3) feeds into Eqs. (1) and (4) directly giving the charm structure function F_2^{c}. In the CGC framework the dipole-proton forward scattering amplitude N can be found by solving BK or JIMWLK evolution equations [8, 9]. Here, we show that the AdS/CFT-inspired color-dipole model of [6] predicts a new scaling behavior for the proton structure function at very small x and Q^2 in a region where there is no experimental data yet and argue that future experimental measurement of F_2 in this region can be used to test the model.

3 AdS/CFT color dipole model to fit to the F_2 data

The forward scattering amplitude N of a $\mathrm{q\bar{q}}$ dipole on a large nuclear target at high-energy for a strongly coupled $\mathcal{N}=4$ SYM theory employing AdS/CFT correspondence was derived in [6] and had been expressed as a function of Bjorken-x and r [10]:

$$N(r,x) = 1-\exp\left[-\frac{\mathcal{A}_0\,x\,r}{\mathcal{M}_0^2(1-x)\pi\sqrt{2}}\times \left(\frac{1}{\rho_{\mathrm{m}}^3}+\frac{2}{\rho_{\mathrm{m}}}-2\mathcal{M}_0\sqrt{\frac{1-x}{x}}\right)\right], \quad (6)$$

with

$$\rho_{\mathrm{m}} = \begin{cases} \left(\dfrac{1}{3m}\right)^{1/4}\sqrt{2\cos\left(\dfrac{\theta}{3}\right)} & : m\leqslant \dfrac{4}{27} \\ \sqrt{\dfrac{1}{3m\Delta}+\Delta} & : m>\dfrac{4}{27} \end{cases},$$

$$\Delta = \left[\frac{1}{2m}-\sqrt{\frac{1}{4m^2}-\frac{1}{27m^3}}\right]^{1/3},$$

$$m = \frac{\mathcal{M}_0^4(1-x)^2}{x^2},\quad \theta=\arccos\left(\sqrt{\frac{27m}{4}}\right), \quad (7)$$

where we defined $\mathcal{A}_0=\sqrt{\lambda_{\mathrm{YM}}}\,\Lambda$. The impact-parameter integrated $\mathrm{q\bar{q}}$ dipole cross-section on a proton target is then related to the dipole amplitude via $\sigma_{\mathrm{q\bar{q}}}(r,x)=\sigma_0\,N(r,x)$.

The saturation scale in AdS/CFT dipole model (6) is then defined as

$$Q_{\mathrm{s}}^{\mathrm{AdS}}(x)= \frac{2\,\mathcal{A}_0\,x}{\mathcal{M}_0^2(1-x)\pi}\left(\frac{1}{\rho_{\mathrm{m}}^3}+\frac{2}{\rho_{\mathrm{m}}}-2\mathcal{M}_0\sqrt{\frac{1-x}{x}}\right). \quad (8)$$

Note that the AdS/CFT dipole scattering amplitude N from Eq. (6) with the saturation scale from Eq. (8) exhibits the property of geometric scaling [11]: it is a function of $r\,Q_{\mathrm{s}}^{\mathrm{AdS}}(\mathrm{x})$ only, $N(r,x)=1-\exp[-r\,Q_{\mathrm{s}}^{\mathrm{AdS}}(x)/(2\sqrt{2})]$.

We fit the AdS/CFT color-dipole parametrization to the experimental data on the proton structure function $F_2(x,Q^2)$ measured by ZEUS [12] at HERA in the kinematical region $x<6\times10^{-5}$ and $Q^2<2.5\ \mathrm{GeV}^2$. As λ_{YM} and Λ only appear together in $\mathcal{A}_0$ we put $\Lambda=1$ GeV throughout this paper examine different cases with fixed $\lambda_{\mathrm{YM}}=10,20,30$. The other two free parameters $\mathcal{M}_0$ and σ_0 in the AdS/CFT dipole model will be determined from a fit to the data. The results of the fit is presented in Table. 1. The first three lines and the last two lines in Table. 1 show the results without and with the presence of the charm quark contribution to F_2. In the fit we adopt light quark mass $m_{\mathrm{u}}=m_{\mathrm{d}}=m_{\mathrm{s}}=140$ MeV and charm quark mass $m_{\mathrm{c}}=1.4$ GeV.

Table 1. Parameters of the AdS/CFT dipole model from Eq. (6) determined from a fit to F_2 data reported by ZEUS.

m_c/GeV	$\lambda_{\rm YM}$	$\mathcal{M}_0(10^{-3})$	σ_0/mb	χ^2/d.o.f.
–	10	8.16	26.08	0.82
–	20	6.54	22.47	0.92
–	30	5.72	20.80	0.98
1.4	10	7.66	24.72	1.03
1.4	20	6.16	21.31	1.18

We checked that the quality of the fit based on the AdS/CFT color-dipole model is very sensitive to the upper bound of the given Bjorken-x bin. Note that currently there is no experimental data below the lower x and Q^2 bound we have taken, and also there are no experimental data for F_2 at large Q^2 but very small x. While the smaller values of $\lambda_{\rm YM}$ appear to give better description of the F_2 data using our AdS/CFT ansatz, one has to keep in mind that AdS/CFT correspondence is valid for $\lambda_{\rm YM} \gg 1$. We therefore can not use very small $\lambda_{\rm YM}$ in the fit, as the whole underlying theoretical approach of [6] would reach its limit of applicability.

In Fig. 1, we show the description of the proton structure function F_2 obtained from the fit for the AdS/CFT and the GBW dipole model [7]. The curves showed at $x < 10^{-6}$ are our predictions of F_2 for this region. Notice that although both models give a good fit of existing data, they lead to drastically different predictions for the structure function at smaller x in the region where there is no experimental data yet. The main prediction of the AdS/CFT color-dipole model is that at very small x it gives rise to a saturating behavior of the structure function which becomes independent of x. The onset of this limiting (scaling) behavior moves to a smaller x for larger Q^2.

One can also apply the fitted parameters given in Table. 1 to predict the longitudinal structure function $F_{\rm L}$, charm structure function $F_2^{\rm c}$ in the kinematic regions of future experiments. The detailed calculations and the results can be found in Ref. [10]. In [10] we also fitted the s-dependent dipole amplitude $N(r,s)$ [8] to the HERA data at small x and Q^2, and calculated the total photo-production cross-sections as a function of $\sqrt{s}$.

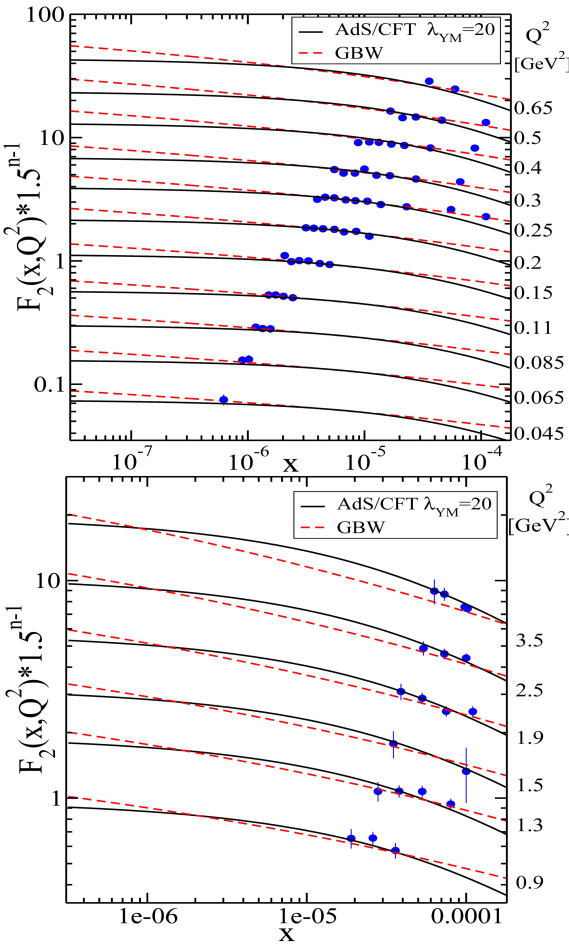

Fig. 1. Results of our AdS/CFT-based fit to the proton structure function F_2 for the AdS/CFT and GBW dipole models, respectively.

In the left panel of Fig. 2 we plot the AdS/CFT dipole cross-section as a function of the dipole transverse size r. It is obvious that AdS/CFT dipole cross-section profile saturates for $x < 10^{-8}$ and will not change further with x. In the right panel of Fig. 2 we show the saturation scale for both the AdS/CFT and the GBW dipole models. It can be seen that the saturation scale in AdS/CFT dipole model is smaller than the one obtained from the GBW model at very small x. Moreover, the AdS/CFT model of [6] predicts that the saturation scale saturates. The saturation scale in the AdS/CFT dipole model defined via Eq. (8) is proportional to $\sqrt{\lambda_{\rm YM}}/\mathcal{M}_0^2$. Therefore, smaller $\lambda_{\rm YM}$ leads to a smaller saturation scale.

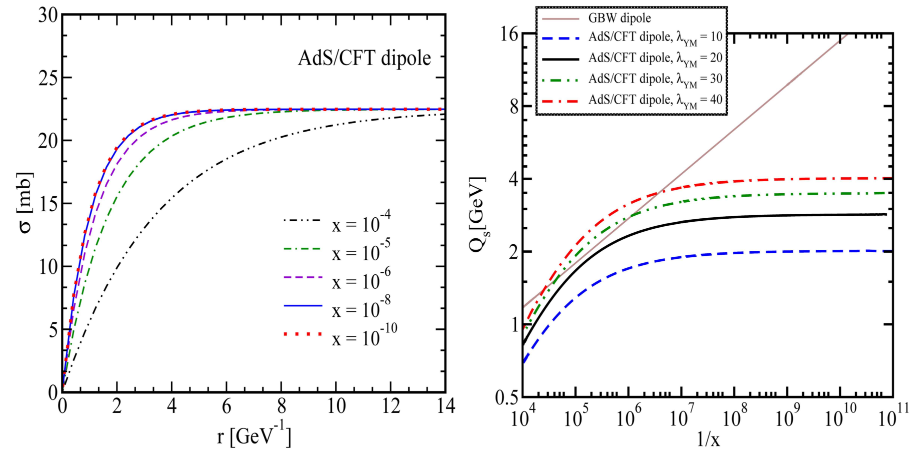

Fig. 2. Left panel: the AdS/CFT dipole cross-section obtained from the fit given in Table. 1 for $\lambda_{\rm YM} = 20$ at various fixed Bjorken-x as a function of the dipole size r. Right panel: the AdS/CFT and the GBW saturation scales $Q_{\rm s}(x)/{\rm GeV}$ as functions of x.

References

1 Gribov L V, Levin E M, Ryskin M G. Phys. Rept, 1983, **100**: 1–150; Mueller A H, QIU J W. Nucl. Phys. B, 1986, **268**: 427–452

2 Kovchegov Y V. Phys. Rev. D, 1999, **60**: 034008; Balitsky I. Nucl. Phys. B, 1996, **463**: 99–160

3 Jalilian-Marian J, Kovner A, Leonidov A, H Weigert. Nucl. Phys. B, 1997, **504**: 415–431; Iancu E., Leonidov A., McLerran L. D. Nucl. Phys. A, 2001, **692**: 583–645

4 Iancu E, Itakura K, McLerran L D. Nucl. Phys. A, 2002, **708**: 327–352

5 Maldacena J M. Adv. Theor. Math. Phys. 1998, **2**: 231–252

6 Albacete J L, Kovchegov Y V, Taliotis A. JHEP, 2008, **0807**: 074

7 Golec-Biernat K, Wüsthoff M. Phys. Rev. D, 1999, **59**: 014017; Phys. Rev. D, 1999, **60**: 114023

8 Albacete J L, Armesto N, Milhano J G, Salgado C A. Phys. Rev. D, 2009, **80**: 034031

9 Lublinsky M, Gotsman E, Levin E Maor U. Nucl. Phys. A, 2001, **696**: 851–869

10 Kovchegov Y V, LU Z, Rezaeian A H. Phys. Rev. D, 2009, **80**: 074023

11 Stasto A M, Golec-Biernat K, Kwiecinski J. Phys. Rev. Lett., 2001, **86**: 596–599

12 Breitweg J et al (ZEUS collaboration). Phys. Lett. B, 2000, **487**: 53–73; Chekanov S et al (ZEUS collaboration). Eur. Phys. J. C, 2001, **21**: 443–471